




Article

# Cloaking Using the Anisotropic Multilayer Sphere

Sidra Batool <sup>1,\*</sup> , Mehwish Nisar <sup>1</sup>, Fabrizio Frezza <sup>1</sup>  and Fabio Mangini <sup>2</sup> 

<sup>1</sup> Department of Information Engineering, Electronics, and Telecommunications, “La Sapienza” University of Rome, Via Eudossiana 18, 00184 Rome, Italy; mehwish.nisar@uniroma1.it (M.N.); fabrizio.frezza@uniroma1.it (F.F.)

<sup>2</sup> Department of Information Engineering, University of Brescia, Via Branze 59, 25123 Brescia, Italy; fabio.mangini@unibs.it

\* Correspondence: sidra.batool@uniroma1.it

Received: 13 June 2020; Accepted: 23 July 2020; Published: 26 July 2020



**Abstract:** We studied a Spherically Radially Anisotropic (SRA) multilayer sphere with an arbitrary number of layers. Within each layer permittivity components are different from each other in radial and tangential directions. Under the quasi-static approximation, we developed a more generalized mathematical model that can be used to calculate polarizability of the SRA multilayer sphere with any arbitrary number of layers. Moreover, the functionality of the SRA multilayer sphere as a cloak has been investigated. It has been shown that by choosing a suitable contrast between components of the permittivity, the SRA multilayer sphere can achieve threshold required for invisibility cloaking.

**Keywords:** anisotropic material; cloaking; polarizability; quasi-static model

## 1. Introduction

Recently, electromagnetic cloaking has achieved great progress theoretically as well as experimentally. In addition to the optical regime [1–4], many applications have been considered for the microwave range of spectrum [3]. The first approach in this respect was the use of coordinate transformation to control electromagnetic waves. In this method, the object that has to be cloaked is virtually transformed into a point or a line. Using this transformation, the parameters required for cloaking coating, i.e., permittivity and permeability, have been derived. Based on transformation optics, the design of spherical cloak with isotropic multilayers has also been proposed [5].

Alternatively, another approach, called scattering cancellation and basic principle of scattering has been proposed [6–10]. This cloaking technique requires plasmonic metamaterials as a cloak medium. The scattering cancellation mechanism is very specific about the dimensions and material of the target object. The object dimension has to be small compared to operating wavelength, in other words, it can cancel the dominant scattering mode under quasi-static condition.

Radially-dependent cloaking methods using anisotropic shells and coatings have also been investigated and employed for spherical and cylindrical shaped geometries [11–13]. Based on Mie theory, cloaking models using multilayer anisotropic spherical shells have also been developed [14,15]. Under full-wave analysis, the analytical solution of electromagnetic (EM) scattering by radially multilayered uniaxial anisotropic spheres placed in free space and all the field expansion coefficients are expressed in the form of spherical vector wave functions [16]. However, only the EM scattered by multilayered uniaxial anisotropic spheres is characterized and illustrated.

Motivated by Pendry’s cloak for perfect invisibility, the interaction of electromagnetic waves with a coated anisotropic sphere, having radially anisotropic permittivity, as well as permeability, have been studied [13]. An effective medium theory for radially-anisotropic magnetodielectric coated spheres is proposed by Gao et al. [17]. They derive the wave equations for the coated sphere with dielectric and magnetic anisotropies in both the core and the shell. The scattering problem of an anisotropic

sphere has been studied numerically and analytically for parametric studies using the concept of anisotropy ratio [18]. Kettunen et al. [19] have investigated how to achieve cloaking and magnification using a single anisotropic cylindrical and spherical layer based on anisotropy ratio. Naqvi et al. [20] considered this approach under the regime of non-integer dimensional space.

More recently, the concept of mantle cloaking based on the concept of cloaking by surface has been presented in order to overcome the strict limitations and requirements that are mandatory for metamaterial cloaking [7,21]. Theoretical investigations of this cloaking technique with ideal assumptions as well as robust practical designs for 1-D, 2-D and 3-D geometries within FSS technology have also been developed [21]. The idea and practical realization of a broadband mantle cloak, formed by a subwavelength metasurface with both time- and frequency-domain analysis is proposed [22]. It is shown that drastic scattering reduction is achievable over a broad frequency range using active non-Foster mantle cloak.

In this article, we present the model that calculates the effective permittivity and polarizability of a multilayer anisotropic sphere using the transmission line method under the quasi-static limit. When the condition of quasi-static approximation cases, the multipolar effects between the various anisotropic layers that form the spherical structure can no longer be overlooked. Due to these multipolar effects, several resonance peaks will occur at various wavelengths which depend on the thickness and material of the layers, making the anisotropic multilayer structure actually visible. Each layer has been considered as a different region and as having a distinct value of tensor permittivity. Laplace’s equation has been solved for each region and an analytic solution has been derived in the form of potential. It is considered that all permittivity components are positive and the whole structure is placed in free space with vacuum permittivity  $\epsilon_0$ . It has been shown that the whole structure can work as a cloak based on the contrast between radial and tangential permittivity components. All the solutions have been performed up to three layers and obtained results are in good agreement with previously presented works [23,24].

## 2. Formation

Let us consider a multilayer anisotropic sphere with radius  $a_k$  surrounding the isotropic inner core of the sphere shown in Figure 1. The radius of the outer layer is fixed and equal to  $a_1$  and the internal radii may be written as [23,25].

$$a_k = \frac{N - (k - 1)}{N} a_1 \tag{1}$$

The number of layers,  $N$  is an arbitrary number whereas  $k = 1, 2, 3, \dots, N$ .

With excitation from external electric field  $\mathbf{E} = \hat{\mathbf{z}}_0 E$ , the solution that satisfies Laplace’s equation in an arbitrary  $k_{th}$  region isotropic layer can be written as [19,26,27]

$$\Phi_k = B_k r \cos \phi + C_k r^{-2} \cos \phi, \tag{2}$$

whereas, for SRA layer, we obtained

$$\Phi_k = B_k r^{\nu_k} \cos \phi + C_k r^{-\nu_k - 1} \cos \phi \tag{3}$$

and:

$$\nu = \frac{1}{2} \left( -1 + \sqrt{1 + \frac{\epsilon_t}{\epsilon_r}} \right), \tag{4}$$

where  $\epsilon_t$  and  $\epsilon_r$  corresponds to the tangential and radial permittivity components, respectively.

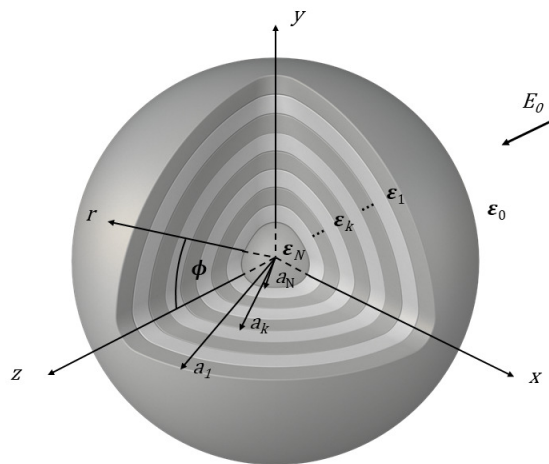


**Figure 1.** Geometry represents the anisotropic multilayer sphere immersed in free space.

Let us consider a geometry composed of a (isotropic to anisotropic) multilayer sphere. Equation (2) represents the potential of  $N$ -layers structure for  $k_{th}$  isotropic subregion, and the consecutive anisotropic layer is

$$\Phi_{k+1} = -B_{k+1}r^{\nu_{k+1}} \cos \phi + C_{k+1}r^{-\nu_{k+1}} \cos \phi. \tag{5}$$

By applying boundary conditions, we have

$$\Phi_k = \Phi_{k+1} \quad r = a_{k+1} \tag{6}$$

$$\epsilon_k \frac{\partial r_k}{\partial r} = \epsilon_{k+1} \frac{\partial r_{k+1}}{\partial r} \quad r = a_{k+1}. \tag{7}$$

The resulting generalized algebraic equations for the case of isotropic-to-anisotropic can be written in a matrix form as [28–31]

$$\begin{pmatrix} B_k \\ C_k \end{pmatrix} = [M_k] \begin{pmatrix} B_{k+1} \\ C_{k+1} \end{pmatrix} \tag{8}$$

where

$$[M_k] = \frac{1}{(\nu_k + 1)\epsilon_k} \begin{pmatrix} M_{k11} & M_{k12} \\ M_{k21} & M_{k22} \end{pmatrix} \tag{9}$$

and:

$$\begin{aligned} M_{k11} &= (2\epsilon_k + \nu_{k+1}\epsilon_{k+1}) a_{k+1}^{\nu_{k+1}-1} \\ M_{k12} &= [-2\epsilon_k + (\nu_{k+1} + 1)\epsilon_{k+1}] a_{k+1}^{-\nu_{k+1}-2} \\ M_{k21} &= (\nu_{k+1}\epsilon_{k+1} - \epsilon_k) a_{k+1}^{\nu_{k+1}+2} \\ M_{k22} &= [\epsilon_k + (\nu_{k+1} + 1)\epsilon_{k+1}] a_{k+1}^{-\nu_{k+1}+1}. \end{aligned}$$

Similarly, the generalized propagation matrix for two adjacent anisotropic layers of the sphere, we obtained

$$\begin{pmatrix} B_k \\ C_k \end{pmatrix} = [P_k] \begin{pmatrix} B_{k+1} \\ C_{k+1} \end{pmatrix} \tag{10}$$

where

$$[P_k] = \frac{1}{(2\nu_k + 1)\varepsilon_k} \begin{pmatrix} P_{k11} & P_{k12} \\ P_{k21} & P_{k22} \end{pmatrix} \tag{11}$$

and:

$$\begin{aligned} P_{k11} &= [(\nu_k + 1)\varepsilon_k + \nu_{k+1}\varepsilon_{k+1}] a_{k+1}^{\nu_{k+1}-\nu_k} \\ P_{k12} &= [(\nu_{k+1} + 1)\varepsilon_{k+1} - (\nu_k + 1)\varepsilon_k] a_{k+1}^{-\nu_{k+1}-\nu_k-1} \\ P_{k21} &= (\nu_{k+1}\varepsilon_{k+1} - \nu_k\varepsilon_k) a_{k+1}^{\nu_{k+1}+\nu_k+1} \\ P_{k22} &= [\nu_k\varepsilon_k + (\nu_{k+1} + 1)\varepsilon_{k+1}] a_{k+1}^{-\nu_{k+1}+\nu_k}. \end{aligned}$$

The generalized propagation matrix for the case of anisotropic-to-isotropic layers is

$$\begin{pmatrix} B_k \\ C_k \end{pmatrix} = [Q_k] \begin{pmatrix} B_{k+1} \\ C_{k+1} \end{pmatrix} \tag{12}$$

where:

$$[Q_k] = \frac{1}{(2\nu_k + 1)\varepsilon_k} \begin{pmatrix} Q_{k11} & Q_{k12} \\ Q_{k21} & Q_{k22} \end{pmatrix} \tag{13}$$

and:

$$\begin{aligned} Q_{k11} &= [(\nu_k + 1)\varepsilon_k + \varepsilon_{k+1}] a_{k+1}^{-\nu_k+1} \\ Q_{k12} &= [2\varepsilon_{k+1} - (\nu_k + 1)\varepsilon_k] a_{k+1}^{-\nu_k-2} \\ Q_{k21} &= (\varepsilon_{k+1} - \nu_k\varepsilon_k) a_{k+1}^{\nu_k+2} \\ Q_{k22} &= (2\varepsilon_{k+1} + \nu_k\varepsilon_k) a_{k+1}^{\nu_k-1}. \end{aligned}$$

When  $\nu_k = \nu_{k+1} = 1$ , all above generalized expressions are reduced into the isotropic multilayer sphere [23].

### 3. Special Cases

Considering all the layers of the structure, we obtain the following relationship

$$\begin{pmatrix} B_0 \\ C_0 \end{pmatrix} = [M] \times \left( \prod_{i=0}^{N-2} [P_i] \right) \times [Q] \begin{pmatrix} B_N \\ 0 \end{pmatrix}. \tag{14}$$

When there is no reflected field  $C$  in the inner region, i.e.,  $C_N = 0$ .

3.1. Case-1 : For Number of Layers (N) = 1

When we considered the case  $N = 1$ , the whole structure is reduced only to innermost layer or core that consists of an isotropic sphere placed in free space and for that  $[P_0] = 1$  and  $[Q] = 1$ . The expression of polarizability may be written as [23].

$$\alpha_P = \frac{3V\epsilon_0}{a_1^3} \frac{M_{21}}{M_{11}}, \tag{15}$$

Where  $V$  is the volume of the sphere ( $V = 4\pi a_1^3/3$ ). From the definition of the polarizability, it is convenient to derive the formula of the effective permittivity of the stratified structure.

$$\epsilon_{eff} = \epsilon_0 + \frac{\frac{\alpha_P}{V}}{1 - \frac{\alpha_P}{3\epsilon_0 V}} \tag{16}$$

The normalized polarizability of a dielectric spherical object in free space, by considering the case  $N = 1$ , we have

$$\alpha_P = 3V\epsilon_0 \frac{(\nu_1\epsilon_1 - \epsilon_0)}{2\epsilon_0 + \nu_1\epsilon_1}. \tag{17}$$

3.2. Case-2 : For Number of Layers (N) = 2

In case of  $N = 2, i = 0, 1, 2, 3, \dots, [P_0] = 1$ , the simplified solution of the above Equation (16) is

$$\begin{pmatrix} B_0 \\ C_0 \end{pmatrix} = [M] \times [Q] \begin{pmatrix} B_2 \\ 0 \end{pmatrix}, \tag{18}$$

where

$$[S] = [M] \times [Q] = \frac{1}{3\epsilon_0} \begin{pmatrix} M_{11} & M_{12} \\ M_{21} & M_{22} \end{pmatrix} \times \frac{1}{(2\nu_1 + 1)\epsilon_1} \begin{pmatrix} Q_{11} & Q_{12} \\ Q_{21} & Q_{22} \end{pmatrix}. \tag{19}$$

So, we have the polarizability of two concentric anisotropic sphere

$$\alpha_P = \frac{3\epsilon_0 V}{a_1^3} \frac{S_{21}}{S_{11}} \tag{20}$$

and:

$$\begin{aligned} S_{11} &= \frac{1}{3(2\nu_1 + 1)\epsilon_0\epsilon_1} (M_{11}Q_{11} + M_{12}Q_{21}) \\ S_{12} &= \frac{1}{3(2\nu_1 + 1)\epsilon_0\epsilon_1} (M_{11}Q_{12} + M_{12}Q_{22}) \\ S_{21} &= \frac{1}{3(2\nu_1 + 1)\epsilon_0\epsilon_1} (M_{21}Q_{11} + M_{22}Q_{21}) \\ S_{22} &= \frac{1}{3(2\nu_1 + 1)\epsilon_0\epsilon_1} (M_{21}Q_{12} + M_{22}Q_{22}). \end{aligned}$$

The normalized polarizability is

$$\alpha_P = 3 \frac{(\nu_1\epsilon_1 - \epsilon_0) [\epsilon_2 + (\nu_1 + 1)\epsilon_1] + [\epsilon_0 + (\nu + 1)\epsilon_1] (\epsilon_2 - \nu_1\epsilon_1) (a_2/a_1)^{2\nu_1+1}}{(2\epsilon_0 + \nu_1\epsilon_1) [\epsilon_1(\nu_1 + 1) + \epsilon_2] + [(\nu_1 + 1)\epsilon_1 - 2\epsilon_0] (\epsilon_2 - \nu_1\epsilon_1) (a_2/a_1)^{2\nu_1+1}}. \tag{21}$$

The corresponding polarizability of a homogeneous dielectric sphere with relative permittivity  $\epsilon_h$  is

$$\alpha_p = 3 \frac{(\epsilon_h - 1)}{(\epsilon_h + 1)}. \tag{22}$$

Hence, the effective permittivity  $\epsilon_{eff,p}$  for the sphere may be written as

$$\alpha_p = 3 \frac{(\epsilon_{eff,p} - 1)}{(\epsilon_{eff,p} + 1)}, \tag{23}$$

where

$$\epsilon_{eff,p} = \frac{\epsilon_1 \nu_1 [\epsilon_1 (\nu_1 + 1) + \epsilon_2] + \epsilon_1 (\nu_1 + 1) (\epsilon_2 - \nu_1 \epsilon_1) \left(\frac{a_2}{a_1}\right)^{2\nu_1 - 1}}{[\epsilon_1 (\nu_1 + 1) + \epsilon_2] - (\epsilon_2 - \epsilon_1 \nu_1) \left(\frac{a_2}{a_1}\right)^{2\nu_1 - 1}}. \tag{24}$$

### 3.3. Case-3 : For Number of Layers (N) = 3

For the case  $N = 3$ , the simplified algebraic equation may be written as

$$\begin{pmatrix} B_0 \\ C_0 \end{pmatrix} = [M] \times [P_1] \times [Q] \begin{pmatrix} B_3 \\ C_3 \end{pmatrix}, \tag{25}$$

where

$$[M] \times [P_1] \times [Q] = \frac{1}{3\epsilon_0} \begin{pmatrix} M_{11} & M_{12} \\ M_{21} & M_{22} \end{pmatrix} \times \frac{1}{(2\nu_1 + 1)\epsilon_1} \begin{pmatrix} P_{11} & P_{12} \\ P_{21} & P_{22} \end{pmatrix} \times \frac{1}{(2\nu_2 + 1)\epsilon_2} \begin{pmatrix} Q_{11} & Q_{12} \\ Q_{21} & Q_{22} \end{pmatrix}. \tag{26}$$

The derived expression with many products can be made more convenient by introducing an arbitrary variable  $R$ , so

$$[R] = [M] \times [P_1] \times [Q] \tag{27}$$

and:

$$\begin{aligned} R_{11} &= \frac{1}{3(2\nu_1 + 1)(2\nu_2 + 1)\epsilon_0\epsilon_1\epsilon_2} \left\{ (M_{11}P_{11} + M_{12}P_{21})Q_{11} + (M_{11}P_{12} + M_{12}P_{22})Q_{21} \right\} \\ R_{12} &= \frac{1}{3(2\nu_1 + 1)(2\nu_2 + 1)\epsilon_0\epsilon_1\epsilon_2} \left\{ (M_{11}P_{11} + M_{12}P_{21})Q_{12} + (M_{11}P_{12} + M_{12}P_{22})Q_{22} \right\} \\ R_{21} &= \frac{1}{3(2\nu_1 + 1)(2\nu_2 + 1)\epsilon_0\epsilon_1\epsilon_2} \left\{ (M_{21}P_{11} + M_{22}P_{21})Q_{11} + (M_{21}P_{12} + M_{22}P_{22})Q_{21} \right\} \\ R_{22} &= \frac{1}{3(2\nu_1 + 1)(2\nu_2 + 1)\epsilon_0\epsilon_1\epsilon_2} \left\{ (M_{21}P_{11} + M_{22}P_{21})Q_{12} + (M_{21}P_{12} + M_{22}P_{22})Q_{22} \right\}. \end{aligned}$$

Moreover, the normalized polarizability is

$$\alpha_p = \frac{3V\epsilon_0}{a_1^3} \frac{R_{21}}{R_{11}} \tag{28}$$

where

$$\alpha_P = 3 \frac{(A_1 A_2 A_3) + (A_4 A_5 A_3) \left(\frac{a_2}{a_1}\right)^{2\nu_1+1} + (A_1 A_6 A_7) + (A_4 A_8 A_7) \left(\frac{a_2}{a_1}\right)^{2\nu_1+1} \left(\frac{a_3}{a_2}\right)^{2\nu_2+1}}{(A_9 A_2 A_3) + (A_{10} A_5 A_3) \left(\frac{a_2}{a_1}\right)^{2\nu_1+1} + (A_9 A_6 A_7) + (A_8 A_7 A_{11}) \left(\frac{a_2}{a_1}\right)^{2\nu_1+1} \left(\frac{a_3}{a_2}\right)^{2\nu_2+1}} \quad (29)$$

and:

$$\begin{aligned} A_1 &= \nu_1 \varepsilon_1 - \varepsilon_0 \\ A_2 &= \nu_2 \varepsilon_2 + (\nu_1 + 1) \varepsilon_1 \\ A_3 &= (\nu_2 + 1) \varepsilon_2 + \varepsilon_3 \\ A_4 &= \varepsilon_0 + (\nu_1 + 1) \varepsilon_1 \\ A_5 &= \nu_2 \varepsilon_2 - \nu_1 \varepsilon_1 \\ A_6 &= (\nu_2 + 1) \varepsilon_2 - (\nu_1 + 1) \varepsilon_1 \\ A_7 &= \varepsilon_3 - \nu_2 \varepsilon_2 \\ A_8 &= \nu_1 \varepsilon_1 + (\nu_2 + 1) \varepsilon_2 \\ A_9 &= \nu_1 \varepsilon_1 + 2\varepsilon_0 \\ A_{10} &= (\nu_1 + 1) \varepsilon_1 - 2\varepsilon_0 \\ A_{11} &= (\nu_1 + 1) \varepsilon_1 - 2\varepsilon_0 \\ A_{12} &= \varepsilon_1 (\nu_1 + 1). \end{aligned}$$

So, for the next iteration  $N = 3$ , the effective permittivity  $\varepsilon_{eff,p}$  for the sphere may be written as

$$\varepsilon_{eff,p} = \frac{\nu_1 \varepsilon_1 [(A_2 A_3) + A_{12} (A_5 A_3)] \left(\frac{a_2}{a_1}\right)^{2\nu_1+1} + \nu_1 \varepsilon_1 [(A_6 A_7) + A_{12} (A_8 A_7)] \left(\frac{a_2}{a_1}\right)^{2\nu_1+1} \left(\frac{a_3}{a_2}\right)^{2\nu_2+1}}{(A_2 A_3 - A_5 A_3) \left(\frac{a_2}{a_1}\right)^{2\nu_1+1} + (A_6 A_7 - A_7 A_8) \left(\frac{a_2}{a_1}\right)^{2\nu_1+1} \left(\frac{a_3}{a_2}\right)^{2\nu_2+1}}. \quad (30)$$

#### 4. Multilayer Sphere as a Cloak

If we want to obtain a design rule for an ideal cloak, that is  $\varepsilon_{eff} = 1$ , which is already given in the literature. We are considering a simpler approximative approach if the radius of the inner sphere vanishes. We are using these approximations in effective permittivities for every iteration,  $k \rightarrow N$  and  $a_k \rightarrow 0$ . Consider the iterative case of  $N = 2$ , the radius of the inner core of the sphere i.e.,  $a_2 = 0$ . Inserting this into Equation (25)

$$\varepsilon_{eff,p} \rightarrow \varepsilon_{1r} \nu_1. \quad (31)$$

By choosing the anisotropy components such that

$$\varepsilon_{1t} = \kappa_1, \quad \varepsilon_{1r} = \frac{1}{2\kappa_1 - 1} \quad (32)$$

and then these chosen values are inserted into Equation (25). The resulting anisotropy ratio will be  $\frac{\varepsilon_{1t}}{\varepsilon_{1r}} = \kappa_1 (2\kappa_1 - 1)$ . For growing  $\kappa$ ,  $\nu_1 \rightarrow \infty$  which implies

$$\varepsilon_{eff,p} \rightarrow 1. \quad (33)$$

It shows that the SRA sphere works as a cloak. Similarly, for the case of  $N = 3$ , radius of the inner core  $a_3 = 0$  by using the above Equation (31), we have

$$\varepsilon_{eff,p} = \varepsilon_{2r} \nu_2, \quad (34)$$

which implies

$$\varepsilon_{2t} = \kappa_2, \quad \varepsilon_{2r} = \frac{1}{2\kappa_2 - 1}. \tag{35}$$

Let us choose the permittivity components that satisfy the invisibility condition for an arbitrary  $k_{th}$  number of layers.

$$\varepsilon_{t_k} = \kappa_k, \quad \varepsilon_{r_k} = \frac{1}{2\kappa_k - 1}. \tag{36}$$

### 5. Numerical Results and Discussion

In our manuscript, we numerically investigated the two different aspects of the multilayer anisotropic homogenization model. In the first part, we observed that the normalized polarizability is a function of the N number of layers of the structure. For that, we plotted (18), (22) and (30). During our numerical test, we took the radius of an inner isotropic core equal  $a_1 = 1$ , first anisotropic shell  $a_2 = 0.5$ , second anisotropic shell  $a_3 = 0.25$ . We used three layers derivation of the multilayer anisotropic model surrounding an isotropic core layer. For the validation of this model, we took the anisotropy ratio, it is  $\nu = \{2, 3\}$  such that, for two concentric SRA layers of the structure is  $\nu_1 = 2$  and  $\nu_2 = 3$  and vice versa. We fixed the following value of permittivities are  $\varepsilon = \{1, 2, 4, 6\}$ . It has been used for a number of layers  $N = \{1, 2, 3\}$ , it has also been observed, that the polarizability of the spherical dielectric core, first and the second anisotropic shell is  $a_p = 6.283$ ,  $a_p = 1.500$  and  $a_p = 1.189$ , respectively, shown in Figure 2. Numerical results show the trend of the normalized polarizability approaches zero by increasing the number of anisotropic layers.

In Figure 3, we described the behavior of inhomogeneous isotropic multilayer sphere. In this case, when permittivity of inner layer  $\varepsilon_1 = 2$  and permittivity of cover layer  $\varepsilon_2 = 4$ , polarizability has more weight as compared to the other case, when permittivities of cover and inner layers are  $\varepsilon_2 = 2$  and  $\varepsilon_1 = 4$  respectively. Hence, with an increasing number of layers in both cases polarizability approaches to a negative value. When  $N = 2$ , a similar pattern has been observed for both cases of outer layer permittivity,  $\varepsilon_2 = 4$  and  $\varepsilon_2 = 2$ , respectively. We will continue inspecting this model of inhomogeneous multilayer anisotropic sphere for cloaking applications.

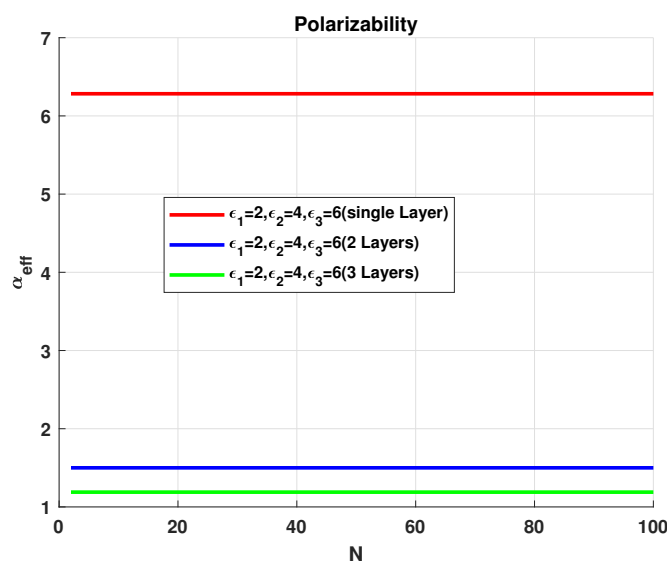


**Figure 2.** Normalized polarizability of isotropic core surrounded by the Spherically Radially Anisotropic (SRA) layers as a function of N number of layers, with the following parameters:  $\varepsilon_1 = 2$ ;  $\varepsilon_2 = 4$ ;  $\varepsilon_3 = 6$ ; and anisotropic ratio is  $\nu_1 = 1$  and  $\nu_2 = 3$ .



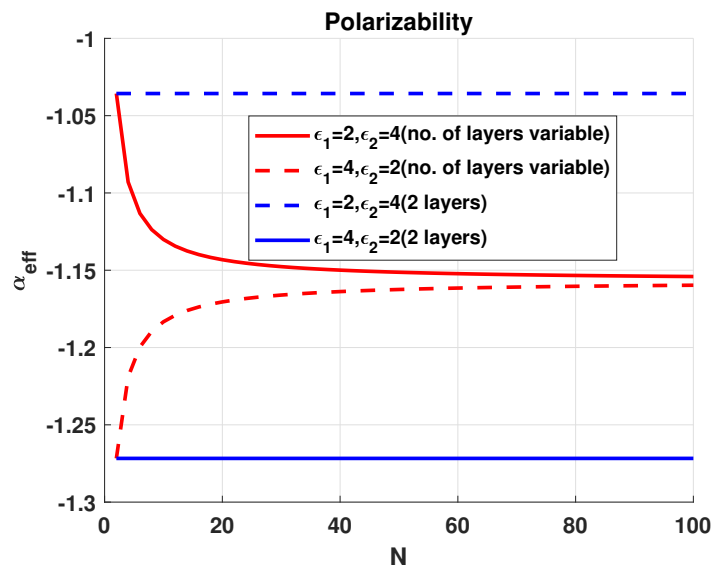


**Figure 3.** Normalized polarizability of the isotropic multilayer sphere as a function of the N number of layers, with the following parameters:  $\epsilon_1 = 2$ ;  $\epsilon_2 = 4$ ;  $\nu_1 = 1$  and  $\nu_2 = 1$ .

In the second part, we investigated the cloaking behavior using anisotropic multilayer sphere. For the validation of this model, we took into account Equation (37) that shows the relationship between radial and tangential permittivity components required for invisibility cloaking. Both components were defined as functions of  $\kappa$ . The permittivity ratio becomes  $\frac{\epsilon_t}{\epsilon_r} = \kappa(2\kappa - 1)$ . The invisibility cloaking condition is  $\frac{\epsilon_t}{\epsilon_r} \rightarrow \infty$ , whereas  $\kappa \rightarrow \infty$ . When we studied simultaneously increasing tangential permittivities and decreasing radial permittivities, it worked like an ideal cloak shown in Figure 4.

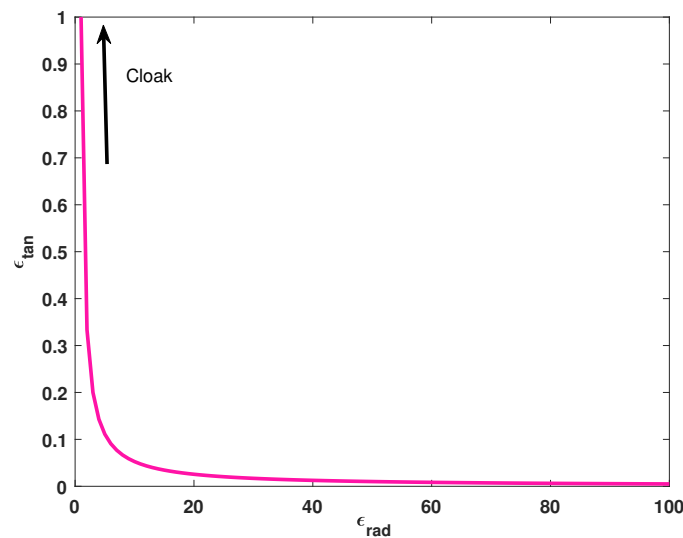


**Figure 4.** The anisotropy ratios that make the intact radially anisotropic multilayer sphere invisible, Equation (37), plotted on a linear scale.

Moreover, we also studied the coherent vision of the cloaking. We manufactured a model of the isotropic layer that is surrounded by a homogeneous anisotropic multilayer sphere using COMSOL Multiphysics (5.2 version). We described the potential distribution of the structure having different parametric values such as radius of the inner core  $a = 0.25$  m, first shell  $b = 0.5$  m, second shell  $c = 0.75$  m and vice versa. Similarly, the tangential permittivity of the outer shell is  $\epsilon_{1t} = 8$ ; second

shell  $\epsilon_{2t} = 4$ ; dielectric core  $\epsilon_{3t} = 1$ , and the radial permittivity of the outer core is  $\epsilon_{1r} = 0.008$ ; second shell  $\epsilon_{2r} = 0.035$ ; and dielectric core  $\epsilon_{3r} = 1$ .

We selected relatively moderate anisotropy ratios  $\nu = \{15, 4.868\}$  which are required to cloak the inner isotropic core layer of the sphere. Figure 5 represents the potential distribution of the structure in the  $xy$ -plane. The homogeneous multi-anisotropic layer makes the multilayer sphere invisible when observed from the outside. Due to simultaneously large radial and small azimuthal permittivity, the potential has a strong gradient at the origin, the structure is very sensitive to any perturbations near the origin.

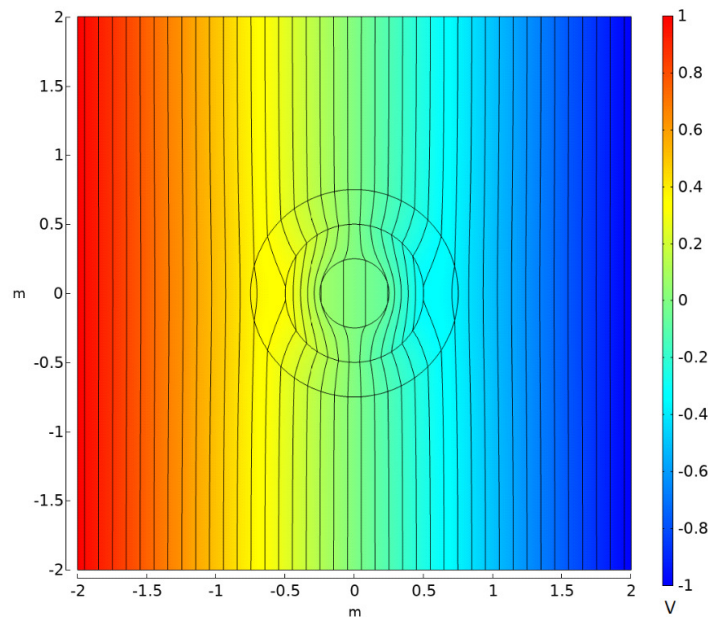


**Figure 5.** Potential distribution of a structure, where anisotropic multilayer sphere with tangential permittivities  $\epsilon_{1t} = \{8, 4, 1\}$  and radial permittivities  $\epsilon_{1r} = \{0.008, 0.035, 1\}$  were taken.

## 6. Conclusions

In this paper, we studied the electrostatic response of the SRA multilayer sphere. A quasi-static mathematical model has been presented that calculates the polarizability and effective permittivity of the SRA multilayer sphere with any arbitrary number of layers. We obtained closed-form expressions for the effective permittivity and consequently, the polarizability. The model has been validated analytically by deriving the results that are already available in the literature for quasi-static approximation. In addition, the working of the SRA multilayer sphere as a cloak has been investigated. Cloaking is based on a certain relationship between radial and tangential permittivity components, that can make the whole structure invisible. Using only a single and thick anisotropic layer around the object that has to be cloaked, it is not possible to have the same value of permittivity everywhere inside the anisotropic shell. In our idea, we discretized a single layer and divided it into a finite number of layers. We assigned different values of permittivity corresponding to each layer and that described the discretization for each layer.

**Author Contributions:** The authors S.B. and M.N. conceived of the presented idea. S.B. developed the formulation or evolution of overarching research goals and aims. and performed the computations. Following co-authors (M.N., F.M., F.F.) encouraged first author to investigate a specific aspect and supervised the findings of this work. All authors provided critical feedback and helped in equal contribution to the formation of the research article. All authors have read and agreed to the published version of the manuscript.

**Funding:** This research received no external funding.

**Conflicts of Interest:** all authors have no conflict of interest.

## References

1. Pendry, J.B.; Schurig, D.; Smith, D.R. Controlling electromagnetic fields. *Science* **2006**, *23*, 1780–1782.
2. Leonhardt, U. Optical conformal mapping. *Science* **2006**, *23*, 1777–1780.
3. Schurig, D.; Mock, J.J.; Justice, B.J.; Cummer, S.A.; Pendry, J.B.; Starr, A.F.; Smith, D.R. Metamaterial electromagnetic cloak at microwave frequencies. *Science* **2006**, *10*, 977–980.
4. Alu, A.; Engheta, N. Theory and potentials of multi-layered plasmonic covers for multi-frequency cloaking. *New J. Phys.* **2008**, *27*, 115–146.
5. Qiu, C.W.; Hu, L.; Xu, X.; Feng, Y. Spherical cloaking with homogeneous isotropic multilayered structures. *New J. Phys.* **2009**, *23*, 602–620.
6. Alu, A.; Engheta, N. Achieving transparency with plasmonic and metamaterial coatings. *Phys. Rev. E* **2005**, *72*, 623–636.
7. Alu, A. Mantle cloak: Invisibility induced by a surface. *Phys. Rev. B* **2009**, *21*, 115–124.
8. Batool, S.; Frezza, F.; Mangini, F.; Xu, Y.L. Scattering from multiple PEC sphere using Translation Addition Theorems for Spherical Vector Wave Function. *J. Quant. Spectrosc. Radiat. Transf.* **2020**, *248*, 106905.
9. Batool, S.; Naqvi, Q.A.; Fiaz, M.A. Scattering from a cylindrical obstacle deeply buried beneath a planar non-integer dimensional dielectric slab using Kobayashi potential method. *Optik* **2018**, *21*, 95–108.
10. Batool, S.; Frezza, F.; Mangini, F.; Simeoni, P.; Introduction of Radar Scattering Application in Remote Sensing and Diagnostics. *Atmosphere*, **2020**, *11*, 1–17.
11. Ni, Y.; Gao, L.; Qiu, C.W. Achieving invisibility of homogeneous cylindrically anisotropic cylinders. *Plasmonics* **2010**, *5*, 251–258.
12. Yu, X.; Gao, L. Nonlinear dielectric response in partially resonant composites with radial dielectric anisotropy. *Phys. Lett. A* **2006**, *4*, 516–522.
13. Chen, H.L.; Gao, L. Anomalous electromagnetic scattering from radially anisotropic nanowires. *Phys. Lett. A* **2012**, *19*, 825–845.
14. Chen, H.; Wu, B.I.; Zhang, B.; Kong, J.A. Electromagnetic wave interactions with a metamaterial cloak. *Phys. Rev. Lett.* **2007**, *6*, 903–920.
15. Cohoon, D.K. An exact solution of Mie type for scattering by a multilayer anisotropic sphere. *J. Electromagnetic Wave* **1989**, *1*, 421–448.
16. Geng, Y.L.; Guo, S.X.; Li, L.W. EM scattering by radially multilayered uniaxial anisotropic spheres. In Proceedings of the 2009 Asia Pacific Microwave Conference, Singapore, 7–10 December 2009; pp. 669–672.
17. Gao, L.; Fung, T.H.; Yu, K.W.; Qiu, C.W. Electromagnetic transparency by coated spheres with radial anisotropy. *Phys. Rev. E* **2008**, *78*, 046–609.
18. Qiu, C.W.; Li, L.W.; Yeo, T.S.; Zouhdi, S. Scattering by rotationally symmetric anisotropic spheres: Potential formulation and parametric studies. *Phys. Rev. E* **2007**, *13*, 209–299.
19. Kettunen, H.; Wallen, H.; Sihvola, A. Cloaking and magnifying using radial anisotropy. *J. Appl. Phys.* **2013**, *28*, 110–124.
20. Nisar, M.; Naqvi, Q.A. Cloaking and magnifying using radial anisotropy in non-integer dimensional space. *Phys. Lett. A* **2018**, *10*, 2055–2060.
21. Chen, P.Y.; Alu, A. Mantle cloaking using thin patterned metasurfaces. *Phys. Rev. B* **2011**, *84*, 205–110.
22. Chen, P.Y.; Argyropoulos, C.; Alu, A. Broadening the cloaking bandwidth with non-Foster metasurfaces. *Phys. Rev. Lett.* **2013**, *111*, 233001.
23. Mangini, F.; Tedeschi, N.; Frezza, F.; Sihvola, A. Homogenization of a multilayer sphere as a radial uniaxial sphere: Features and limits. *J. Electromagn. Wave* **2014**, *28*, 916–913.
24. Mangini, F.; Tedeschi, N.; Frezza, F.; Sihvola, A. Realization of a Radial Uniaxial sphere with a multilayer sphere. In Proceedings of the XXXIth URSI General Assembly and Scientific Symposium (URSI GASS), Beijing, China, 16–23 August 2014; pp. 1–4.
25. Wallen, H.; Kettunen, H.; Sihvola, A. Singularities or emergent losses in radially uniaxial spheres. In Proceedings of the International Symposium on Electromagnetic Theory, Hiroshima, Japan, 20–24 May 2013.
26. Sihvola, A. *Electromagnetic Mixing Formulas and Applications*; The Institution of Electrical Engineers: London, UK, 1999.
27. Mangini, F.; Tedeschi, N.; Frezza, F.; Sihvola, A. Analysis of the polarizability of an array of spherical metallic inclusions in a dielectric host sphere. *J. Opt. Soc. Am. A* **2014**, *31*, 2409–2414.

28. Mangini, F.; Tedeschi, N.; Frezza, F.; Sihvola, A. Electromagnetic interaction with two eccentric spheres. *J. Opt. Soc. Am. B* **2014**, *31*, 783–789.
29. Sihvola, A.; Lindell, I.V. Transmission line analogy for calculating the effective permittivity of mixtures with spherical multilayer scatterers. *J. Electromagn. Wave* **1988**, *2*, 741–756.
30. Frezza, F.; Mangini, F. Electromagnetic scattering of an inhomogeneous elliptically polarized plane wave by a multilayered sphere. *J. Electromagn. Wave* **2016**, *30*, 492–504.
31. Cheng, Y.; Liu, X.J. Three dimensional multilayered acoustic cloak with homogeneous isotropic materials. *J. Appl. Phys. A* **2009**, *94*, 25–30.



© 2020 by the authors. Licensee MDPI, Basel, Switzerland. This article is an open access article distributed under the terms and conditions of the Creative Commons Attribution (CC BY) license (<http://creativecommons.org/licenses/by/4.0/>).